Thin Solid Films 577 (2015) 82–87

Contents lists available at ScienceDirect

Thin Solid Films

journal homepage: www.elsevier.com/locate/tsf

Application of femtosecond laser ablation inductively coupled plasma mass spectrometry for quantitative analysis of thin Cu(In,Ga)Se_2 solar cell films

Seokhee Lee [a], Jhanis J. Gonzalez [b,c], Jong H. Yoo [c], Jose R. Chirinos [b,d], Richard E. Russo [b,c], Sungho Jeong [a,*]

[a] School of Mechatronics, Gwangju Institute of Science and Technology, 1 Oryong-dong, Buk-gu, Gwangju 500-712, Republic of Korea
[b] Lawrence Berkeley National Laboratory, 1 Cyclotron Road, Berkeley, CA 94720, USA
[c] Applied Spectra Inc., 46665 Fremont Boulevard, Fremont, CA 94538, USA
[d] Facultad de Ciencias, Universidad Central de Venezuela, Caracas 1041A, Venezuela

ARTICLE INFO

Article history:
Received 25 August 2014
Received in revised form 23 December 2014
Accepted 15 January 2015
Available online 22 January 2015

Keywords:
Femtosecond
LA-ICP-MS
CIGS
Solar cell
Composition

ABSTRACT

This work reports that the composition of Cu(In,Ga)Se_2 (CIGS) thin solar cell films can be quantitatively predicted with high accuracy and precision by femtosecond laser ablation-inductively coupled plasma-mass spectrometry (fs-LA-ICP-MS). It is demonstrated that the results are strongly influenced by sampling conditions during fs-laser beam ($\lambda = 1030$ nm, $\tau = 450$ fs) scanning on the CIGS surface. The fs-LA-ICP-MS signals measured at optimal sampling conditions generally provide a straight line calibration with respect to the reference concentrations measured by inductively coupled plasma optical emission spectroscopy (ICP-OES). The concentration ratios predicted by fs-LA-ICP-MS showed high accuracy, to 95–97% of the values measured with ICP-OES, for Cu, In, Ga, and Se elements.

1. Introduction

Cu(In,Ga)Se_2 (CIGS) solar cell has many attractive properties such as high cell efficiency (>20%) [1], long-term stability [2], and low manufacturing cost [3], and thus there has been a tremendous research effort to improve the performance of CIGS solar cell. Several factors influence the performance of CIGS thin film solar cell, including optical transmission through the front-contact, material and thickness of the buffer layer, composition of the absorber layer, film growth process, and back-contact material [2,3]. In terms of CIGS film growth, for example, various methods such as a hybrid process combining evaporation and sputtering [4], CIGS nanoparticle-coating [5] and electrodeposition as a nonvacuum process [6] have been attempted in order to achieve a higher quality CIGS as well as lower production cost. The information for structure and surface morphology of CIGS produced with different processes was also of interest [6,7].

Besides the fabrication processes, the composition of major constituent elements (Cu, In, Ga, and Se) of a CIGS film is also known to be a significant factor determining the electrical and optical properties of a CIGS solar cell [8,9]. Accordingly, researches about the analysis of elemental composition of CIGS thin films have been increasing recently. Various analytical techniques such as Auger electron spectroscopy, X-ray photoelectron spectroscopy, energy dispersive X-ray spectrometry, inductively coupled plasma optical emission spectroscopy (ICP-OES), and secondary ion mass spectrometry have been used to analyze the chemical composition of CIGS thin films [10–13]. Depending on the method employed for analysis, however, the accuracy, measurement time, spatial resolution, and availability of the technique differ significantly. In principle, a fast, accurate, and reliable technique that can be readily applied for the evaluation of CIGS solar cell during device development or manufacturing processes is most desired by solar cell researchers and industry [10,14].

The analysis of thin film solar cells is one of the application fields to which the characteristics of laser ablation-inductively coupled plasma-mass spectrometry (LA-ICP-MS) can be effectively applied. LA-ICP-MS is a powerful method for elemental analysis with advantages of real-time analysis [15,16], minimal sample consumption, no sample preparation [17], little waste, and minimal exposure to toxic samples [18]. Accordingly, LA-ICP-MS has been employed in various areas of application such as geochemistry [19], forensic science [20], environmental science [21], semiconductors [22], biomedicine [23], nuclear non-proliferation detection [24], and so forth. The coupling of femtosecond (fs) laser to ICP-MS (fs-LA-ICP-MS) has been demonstrated as one of the most accurate analytical methods due to the capability of near stoichiometric ablation and the generation of mono-disperse nanometer sized particles that can be easily digested in the ICP [18,25,26]. The analytical performance of LA-ICP-MS was significantly enhanced with a fs-laser by

* Corresponding author.
E-mail address: shjeong@gist.ac.kr (S. Jeong).

http://dx.doi.org/10.1016/j.tsf.2015.01.026
0040-6090/

reducing errors related to particle size distribution and matrix dependence [27,28].

In this work, we report the results for fs-LA-ICP-MS analysis of thin CIGS solar cell films. It is shown that the elemental concentrations of CIGS films can be accurately predicted by properly choosing sampling parameters. Calibration curves were generated for the fs-LA-ICP-MS signal ratios of the constituent elements with reference materials that were validated by ICP-OES and their accuracy was analyzed.

2. Experimental details

2.1. CIGS film preparation

The CIGS thin film samples used in experiments were fabricated on soda lime glass (SLG) substrates by a three stage co-evaporation method with 1 μm thick Mo back contact layer. The CIGS thin films were produced with varying Ga/In ratios by controlling Ga and In evaporation fluxes; the detailed fabrication processes of these samples were reported elsewhere [29]. The average composition of fabricated CIGS thin films was then verified by ICP-OES (Verian, 720-ES) for In, Ga and Se, and atomic absorption spectroscopy (Thermo Scientific, iCE 3000) for Cu, and the results are listed in Table 1. The thicknesses of CIGS and Mo layers were measured using scanning electron microscope (SEM) (Hitachi, S-4800, operation voltage = 15 kV) images of a cross section.

2.2. fs-LA-ICP-MS system

A commercial laser ablation system (Applied Spectra Inc., J100, pulse width = 450 fs, wavelength = 1030 nm) coupled to an ICP-MS (Thermo Scientific, XSERIES 2) was used for the fs-LA-ICP-MS measurements. The laser spot diameter and fluence at the sample surface were fixed at about 30 μm and 19.53 J/cm^2, respectively. The CIGS thin film samples were ablated in a chamber to which He was supplied at a flow rate of 0.9 L min^{-1} as a carrier gas. The ablated mass swept by the He gas was then entrained into an Ar make-up gas flowing at the rate of 0.9 L min^{-1}. The experimental settings for the ICP-MS were forward power of 1400 W, Ar flow rates of 13 and 0.7 L min^{-1} for plasma and auxiliary gases, respectively, voltages of −82, −1150, −80, −195 V for the extraction, L1, L2, and L3 lenses. The ICP-MS measurements for six isotopes (^{65}Cu, ^{115}In, ^{71}Ga, ^{82}Se, ^{95}Mo, ^{23}Na) were acquired in the time resolved mode and each ICP-MS response was integrated with background subtraction to obtain the average response per isotope.

3. Results and discussion

3.1. Effects of sampling conditions

During fs-LA-ICP-MS measurements, the ICP-MS response varies sensitively with respect to ablation conditions. Since the laser spot size and energy were fixed by the system during the measurement, laser repetition rate and scan speed were varied in the ranges of 5–500 Hz and 10–500 μm/s, respectively, to examine the effects of ablation conditions. Depending on the combination of repetition rate and scan speed, the number of overlapping pulses on each laser spot changed from zero to about 30 pulses. Fig. 1(a) shows that the integrated counts per second (ICPS) of the four major elements at the conditions of repetition rate of 5 Hz and scan speed of 300 μm/s. At this condition, no overlapping took place between pulses as observed in the cross-sectional profile of craters (inset of Fig. 1(a)) measured using a white light interferometric microscope (Zygo New View 6000) and the crater depth was mostly below 2 μm. Each isotope profile (^{65}Cu, ^{115}In, ^{71}Ga, and ^{82}Se) in Fig. 1(a) represents an accumulated signal from ten ablation spots along the scan direction for which the complete ablation took about 2 s (total ablated volume ≈ 400 μm^3). The ^{23}Na signal is attributed to Na element diffused from soda lime glass during the growth of the CIGS film.

The accuracy and precision of the ICP-MS response shown in Fig. 1(a) are closely related to the ablation conditions. Gonzalez et al. [30] reported that the ICP-MS signal intensity and crater profile differed if the scan speed and repetition rate had changed even at the same number of overlapping pulses. The primary reason for these changes in ICP-MS response is the variation in particle characteristics such as particle size and size distribution sampled during laser–material interactions. The influence of ablation conditions on the analysis performance of

Table 1
Concentration and thickness of the CIGS thin film samples.

Sample No.	Concentration (at.%)				Concentration ratio	Thickness (nm)	
	Cu	In	Ga	Se	Ga/In	CIGS	Mo
1	25.72	23.31	3.05	47.92	0.131	1720	982
2	25.31	20.91	4.82	48.96	0.231	1885	991
3	25.50	19.40	7.41	47.69	0.382	2175	967
4	25.59	16.82	8.16	49.43	0.485	2020	1100
5	25.77	17.27	9.14	47.82	0.529	1885	1085
6	25.43	15.18	10.91	48.49	0.719	1358	1100
7	26.32	13.12	12.97	47.59	0.989	1335	933

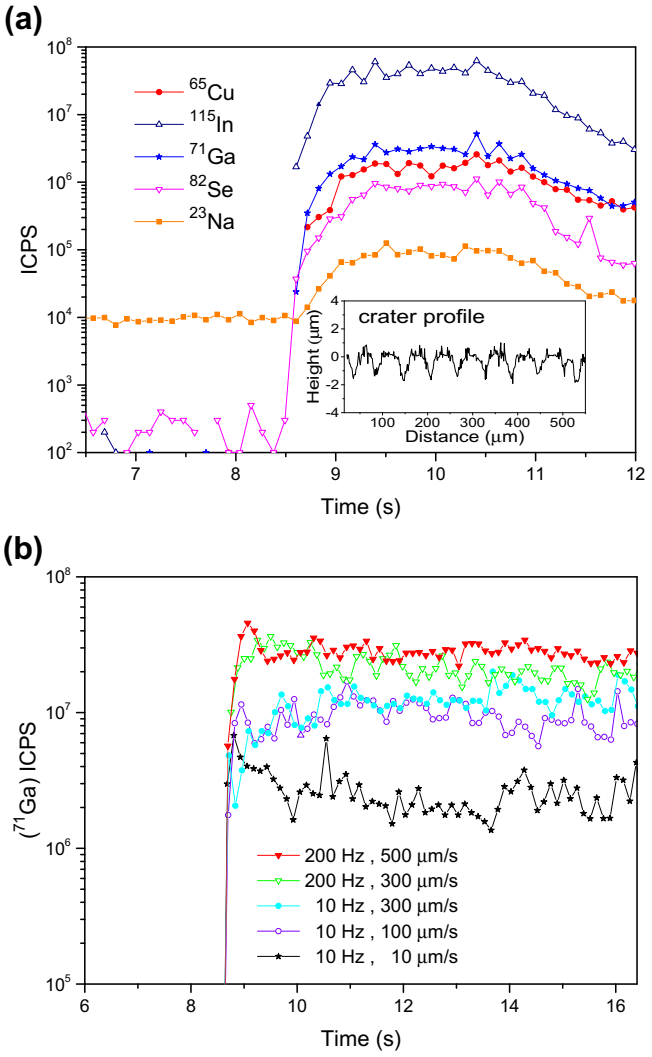

Fig. 1. (a) Transient fs-LA-ICP-MS response during consecutive ablation of ten craters on a CIGS film (Sample No. 3) (repetition rate = 5 Hz, scan speed = 300 μm/s) and (b) ^{71}Ga isotope signals measured at different ablation conditions.

ICP-MS can be examined by calculating temporal relative standard deviation (TRSD) of the ICP-MS response profiles which represents the short-term signal fluctuation on the temporal response [31]. The improvement in TRSD is related to a more consistent particle size distribution and particle chemical composition during repetitive pulsed laser ablation [27]. Fig. 1(b) shows the transient ICP-MS signals of ^{71}Ga measured at different pulse repetition rates and scan speeds. Note that the signal intensity of ^{71}Ga increased with scan speed for the same repetition rate. This result is similar to that by Gonzalez et al. [30] where the low signal intensity at low scan speed for a fixed repetition rate was attributed to the accumulation of particles in front of the surface, decreasing the ablation and/or transport efficiency due to the absorption/diffusion of the laser beam. The signal increase of ^{71}Ga for increasing repetition rate at the fixed scan speed of 300 μm/s may be due to an increased amount of ablated mass. The average ICPS and TRSD of ^{71}Ga calculated at various combinations of scan speed and repetition rate are presented in Fig. 2(a). For the same repetition rate (see the 10 Hz case), the signal intensity and TRSD improved initially for increasing scan speed but became deteriorated for further increase when the signal intensity reached near the maximum. The same trend was observed for the ^{82}Se, as shown in Fig. 2(b). Based on these results, repetition rate of 200 Hz and scan speed of 500 μm/s were selected as the optimal sampling conditions in this study to achieve high ICP-MS signal and low fluctuation.

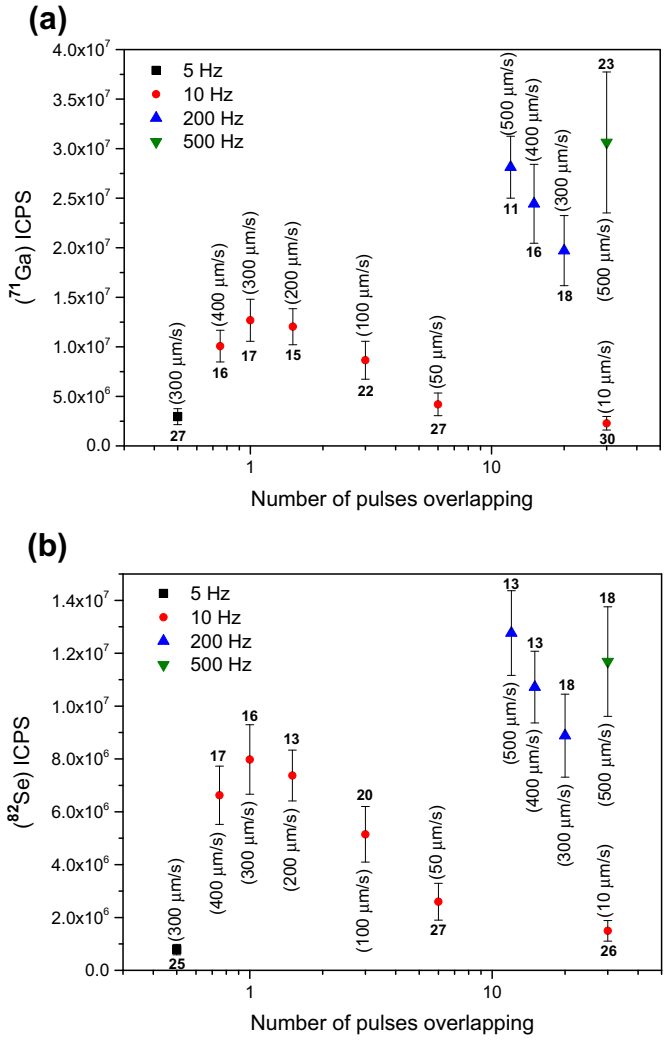

Fig. 2. Variation of ICPS intensity and TRSD of (a) ^{71}Ga and (b) ^{82}Se signals at varying sampling conditions (Sample No. 3) (The values next to a data point represent TRSD and scan speed).

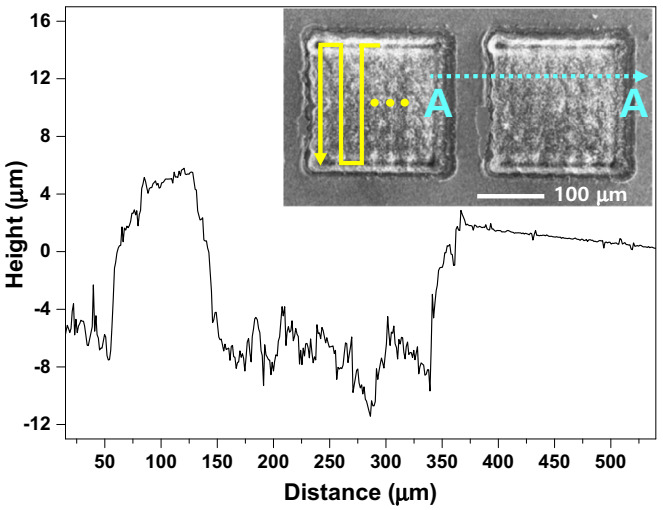

Fig. 3. SEM image of the ablation craters and their cross-sectional profile produced on a CIGS film (Sample No. 3) (repetition rate = 200 Hz, scan speed = 500 μm/s).

3.2. Compositional analysis of CIGS thin film

Fig. 3 shows the ablation craters and cross-sectional crater profile of one of the CIGS solar cell films sampled at the conditions of 200 Hz laser repetition rate and 500 μm/s scan speed. Each sample was scanned by the laser beam in a zig-zag pattern over an area of 200 μm × 200 μm with a line spacing of 14.3 μm. At this condition, the complete ablation of a rectangular crater took about 6.65 s. The cross-sectional profile of the rectangular crater showed that the surface between craters was significantly elevated due to accumulation of ablated particles [30]. Since the thickness of CIGS layer of the sample in Fig. 3 was only about 2.2 μm, the crater depth (>6 μm) sampled not only the CIGS film but also the Mo layer and part of the SLG substrate.

The same fs-LA-ICP-MS measurement was repeated over a 3 × 3 crater array for each CIGS sample and the average from the nine rectangular craters was then used to represent the ICP-MS isotope signal of each sample. Fig. 4 shows the ICP-MS responses of ^{65}Cu, ^{71}Ga, ^{82}Se, and ^{115}In isotopes, representing the four major elements of CIGS solar cell

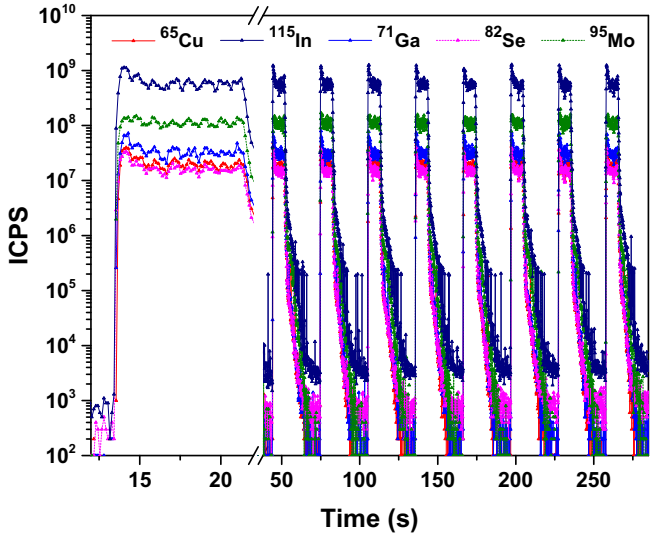

Fig. 4. Transient fs-LA-ICP-MS signals of ^{65}Cu, ^{71}Ga, ^{82}Se, ^{115}In, and ^{95}Mo isotopes during sampling nine rectangular craters (Sample No. 3).

films, from the nine rectangular craters sampled at the laser repetition rate of 200 Hz and scan speed of 500 μm/s. It is observed that the transient responses of ICP-MS are consistent over the nine rectangular craters, which demonstrates that the CIGS thin film had a spatially homogeneous elemental composition. The detailed time response profiles of the ICP-MS can be found from the signals of the first crater in Fig. 4. The measurement of ^{65}Mo in Fig. 4 indicates that the ablation took place not only through the CIGS layer but also into the Mo layer at this condition. The relative standard deviation (RSD) of the ICPS intensities of each isotope signal from the nine craters in Fig. 4 was estimated to be within 1.3–6.8%, implying that highly reproducible measurement can be performed with fs-LA-ICP-MS at the optimal sampling condition. In comparison, when the ablation was carried out at the reduced repetition rate and scan speed of 5 Hz and 300 μm/s, respectively, the conditions at which ablation depth became nearly the same as the CIGS film thickness as shown in the inset of Fig. 1(a), the RSD values of average signals from ten measurements (with ten ablation spots per measurement) increased to the range of 5.8–18.6%. The deterioration of reproducibility at this reduced repetition rate and scan speed is considered to be related to the variation in particle characteristics as discussed above.

Since the thickness of each CIGS sample was different from others as shown in Table 1, the ablated mass of an element from each sample becomes proportional to not only the elemental concentration but also the sample thickness. Thus, absolute ICPS of the ICP-MS isotope signal cannot be directly correlated to the elemental concentration of each sample. Alternatively, since the ICPS ratios between elements should remain proportional to the elemental concentration ratios of each CIGS sample, the measured fs-LA-ICP-MS signal was calibrated with respect to the relative concentrations of constituent elements. Because the concentrations of Cu and Se were almost constant at around 25 at.% and 50 at.%, respectively, among the CIGS solar cell samples, these elements were utilized as the internal standards for the generation of calibration curves. The calibration curve of Ga/In ratio also was established because the Ga/In ratio is a crucial factor determining CIGS solar cell efficiency. Fig. 5 shows the calibration curves for Ga/Cu, In/Cu, Ga/Se, In/Se, and Ga/In established from the ICPS ratio data acquired at the optimal sampling condition. Fig. 5 demonstrates that the obtained calibration curves have a good linear correlation with the ICP-OES measured elemental concentration ratios. The R^2 values of the linear fitting on the calibration curve were close to or over 0.99 except the In/Se ratio (0.96). By taking the ICPS ratios instead of the absolute intensities, the RSD values of the nine measurements decreased to below 2% in average (maximum 3.24% for Ga/Se) as shown in Table 2. These results confirm that fs-LA-ICP-MS measurement provides accurate calibration results for composition analysis of CIGS films.

In order to evaluate the accuracy of predicted concentration, cross-validation was carried out using the measured fs-LA-ICP-MS data as follows [32–34]. For example, to calculate the concentration ratio of Ga/In in sample 1 from the fs-LA-ICP-MS data, the ICP-OES measured concentration ratios of samples 2–7 (y_{2-7}) in Fig. 5(c) were fitted into a linear equation as a function of ICPS ratio (x) ($y_{2-7} = a + bx$), leaving out sample 1. Then, using the $y_{2-7} = a + bx$ equation and measured ICPS ratio of sample 1, the concentration ratio (Ga/In) of sample 1 was predicted and plotted with respect to the concentration measured by ICP-OES. The same procedure was repeated for all samples and the five different calibration curves, and the results are shown in Fig. 6. The closeness of the concentration ratios predicted by cross-validation to the ICP-OES

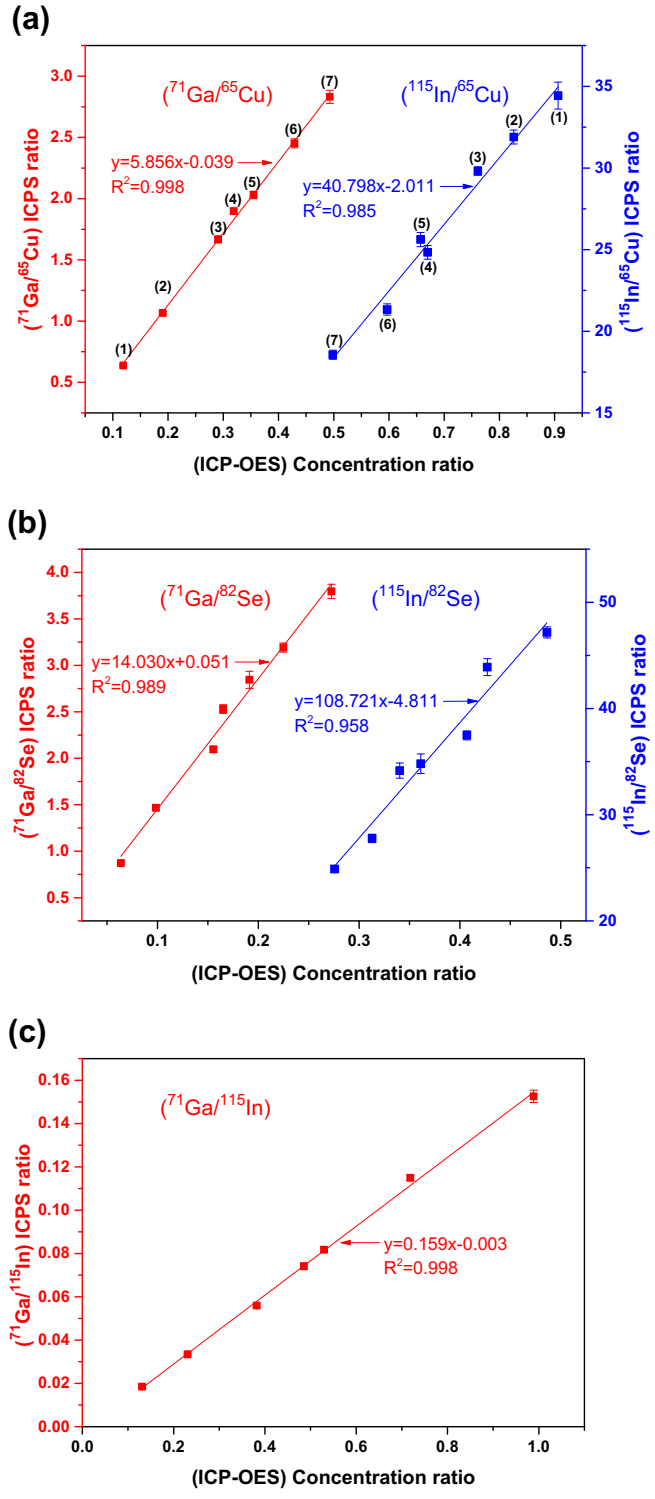

Fig. 5. Calibration curves of ICPS ratios for fs-LA-ICP-MS measurements: (a) Ga/Cu and In/Cu, (b) Ga/Se and In/Se, and (c) Ga/In (The number next to a data point represents sample number).

Table 2
Relative standard deviation of the ICPS ratios for nine measurements.

Sample No.	Relative standard deviation (%)				
	Ga/Cu	In/Cu	Ga/Se	In/Se	Ga/In
1	1.06	2.40	1.85	1.10	2.30
2	1.11	1.34	1.85	1.81	1.48
3	1.66	0.86	1.55	1.12	1.25
4	1.32	1.70	1.83	2.07	2.07
5	1.52	1.69	3.24	2.65	1.38
6	1.49	1.62	1.54	1.42	1.15
7	1.90	1.48	2.00	1.22	1.87
average	1.44	1.58	1.98	1.63	1.64

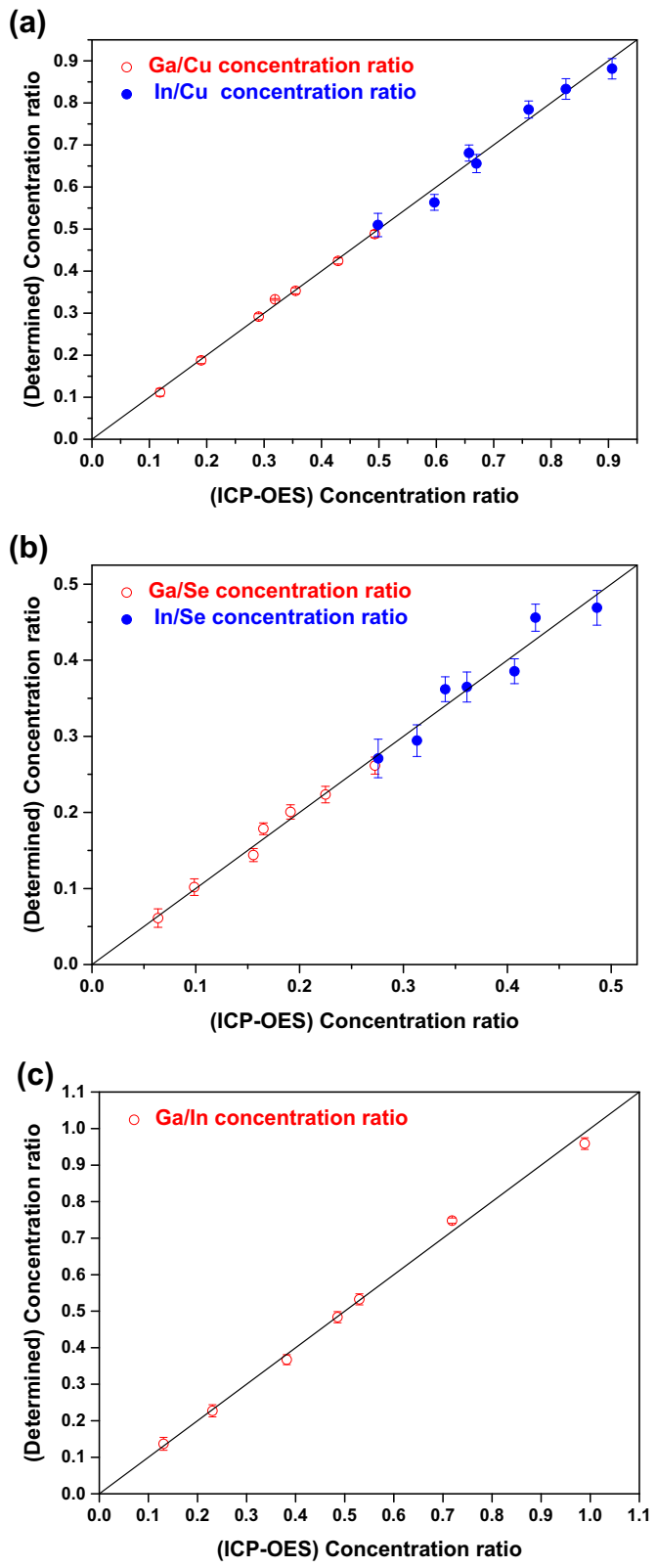

Fig. 6. Cross-validation results of (a) Ga/Cu and In/Cu, (b) Ga/Se and In/Se, and (c) Ga/In concentration ratios predicted by fs-LA-ICP-MS analysis (The diagonal line is for eye guide).

measured values was evaluated from the R^2, slope, and intercept values of the data in Fig. 6 as summarized in Table 3, which should become 1, 1, and 0, respectively, for perfect correlation. Root mean square of relative error (RMSRE) of the calibration curves was also estimated using the following equation [34],

$$RMSRE = \sqrt{\frac{1}{7}\cdot\sum_{i=1}^{7}\left(\frac{C_{ICP\text{-}OES,i}-C_{Determined,i}}{C_{ICP\text{-}OES,i}}\right)^2} \quad (1)$$

where $C_{ICP\text{-}OES}$ is the concentration ratio measured by ICP-OES and $C_{Determined}$ is the concentration ratio predicted through the cross-validation procedures. The results of RMSRE calculation in Table 3 demonstrate that the concentration ratio of any two constituent elements of CIGS thin film can be predicted using fs-LA-ICP-MS with a confidence level of about 95–97% of the ICP-OES measured concentration ratio.

Table 3
Linear fitting parameters and RMSRE of the cross-validation results.

Elemental ratio	R^2	slope	intercept	RMSRE (%)
Ga/Cu	0.997	1.003	−0.002	2.87
In/Cu	0.972	0.981	0.013	3.20
Ga/Se	0.982	0.972	0.004	5.19
In/Se	0.927	0.990	0.003	4.86
Ga/In	0.996	0.985	0.006	2.99

Based on the calibration curves of the ICPS ratio of fs-LA-ICP-MS data, not only the concentration ratios of constituent elements but also the absolute elemental concentration of a CIGS film of unknown composition can be determined quantitatively. Provided that the composition of the CIGS can be represented by the four major elements, ignoring trace elements, such that $x_{Cu} + x_{In} + x_{Ga} + x_{Se} = 100$ where x is the atomic concentration (%) of an element, the absolute concentrations of all four elements can be determined using the calibration curves. At least three of the five calibration curves in Fig. 5 are needed for this purpose. Note that the calibration curves in Fig. 5 are independent of each other. Since the calibration curves for Ga/Cu, Ga/Se, and Ga/In had high linearity and small RMSREs as shown in Fig. 5 and Table 3, these curves may be selected for the prediction. Then, using the x_{Ga}/x_{Cu}, x_{Ga}/x_{Se}, and x_{Ga}/x_{In} values determined from the calibration curves with $x_{Cu} + x_{In} + x_{Ga} + x_{Se} = 100$, the absolute concentration values of the four major elements can be readily obtained.

4. Conclusion

From fs-LA-ICP-MS analysis of CIGS thin films, it is demonstrated that the concentration ratios of constituent elements can be predicted with high accuracy by properly selecting the sampling conditions. At the optimal sampling condition, a highly linear correlation with respect to the original concentration ratio could be achieved. Combined with the intrinsic short measurement time and no necessity of sample preparation, it is considered that fs-LA-ICP-MS can provide a powerful method for fast and quantitative analysis of the major constituent elements of CIGS solar cell films.

Acknowledgment

This work was supported by a National Research Foundation of Korea (NRF) grant funded by the Korea government (Ministry of Education, Science, and Technology) (No. 2013-064113) and RER, XM and JJG acknowledge the support from the Chemical Science Division, Office of Basic Energy Sciences of the U.S. Department of Energy under contract number DE-AC02-05CH11231 at the Lawrence Berkeley National Laboratory.

References

[1] P. Jackson, D. Harishos, E. Lotter, S. Paetel, R. Wuerz, R. Menner, W. Wischmann, M. Powalla, New world record efficiency for Cu(In, Ga)Se_2 thin-film solar cells beyond 20%, Prog. Photovolt. Res. Appl. 19 (2011) 894.

[2] S. Niki, M. Contreras, I. Repins, M. Powalla, K. Kushiya, S. Ishizuka, K. Matsubara, CIGS absorbers and processes, Prog. Photovolt. Res. Appl. 18 (2010) 453.

[3] A. Romeo, M. Terheggen, D. Abou-Ras, D.L. Bätzner, R.J. Haug, M. Kälin, D. Rudmann, A.N. Tiwari, Development of thin-film Cu(In, Ga)Se_2 and CdTe solar cells, Prog. Photovolt. Res. Appl. 12 (2004) 93.

[4] A.E. Delahoy, L. Chen, M. Akhtar, B. Sang, S. Guo, New technologies for CIGS photovoltaics, Sol. Energy 77 (2004) 785.

[5] C.P. Liu, C.L. Chuang, Fabrication of copper–indium–gallium–diselenide absorber layer by quaternary-alloy nanoparticles for solar cell applications, Sol. Energy 86 (2012) 2795.

[6] O. Bamiduro, G. Chennamadhava, R. Mundle, R. Konda, B. Robinson, M. Bahoura, A.K. Pradhan, Synthesis and characterization of one-step electrodeposited $CuIn_{(1-x)}Ga_xSe_2$/Mo/glass films at atmospheric conditions, Sol. Energy 85 (2011) 545.

[7] L.P. Deshmukh, R.V. Suryawanshi, E.U. Masumdar, M. Sharon, $Cu_{1-x}In_xSe_2$ thin films: deposition by spray pyrolysis and characteristics, Sol. Energy 86 (2012) 1910.

[8] M.I. Alonso, M. Garriga, C.A. Durante Rincón, E. Hernández, M. León, Optical functions of chalcopyrite $CuGa_xIn_{1-x}Se_2$ alloys, Appl. Phys. A Mater. Sci. Process. 74 (2002) 659.

[9] S. Theodoropoulou, D. Papadimitriou, K. Anestou, C. Cobet, N. Esser, Optical properties of $CuIn_{1-x}Ga_xSe_2$ quaternary alloys for solar-energy conversion, Semicond. Sci. Technol. 24 (2009) 015014.

[10] D. Abou-Ras, R. Caballero, C.-H. Fischer, C.A. Kaufmann, I. Lauermann, R. Mainz, H. Mönig, A. Schöpke, C. Stephan, C. Streeck, S. Schorr, A. Eicke, M. Döbeli, B. Gade, J. Hinrichs, T. Nunney, H. Dijkstra, V. Hoffmann, D. Klemm, V. Efimova, A. Bergmaier, G. Dollinger, T. Wirth, W. Unger, A.A. Rockett, A. Perez-Rodriguez, J. Alvarez-Garcia, V. Izquierdo-Roca, T. Schmid, P.-P. Choi, M. Müller, F. Bertram, J. Christen, H. Khatri, R.W. Collins, S. Marsillac, I. Kötschau, Comprehensive comparison of various techniques for the analysis of elemental distributions in thin films, Microsc. Microanal. 17 (2011) 728.

[11] H.-R. Hsu, S.-C. Hsu, Y.S. Liu, Improvement of Ga distribution and enhancement of grain growth of $CuInGaSe_2$ by incorporating a thin CuGa layer on the single CuInGa precursor, Sol. Energy 86 (2012) 48.

[12] C. Insignares-Cuello, V. Izquierdo-Roca, J. López-García, L. Calvo-Barrio, E. Saucedo, S. Kretzschmar, T. Unold, C. Broussillou, T. Goislard de Monsabert, V. Bermudez, A. Pérez-Rodríguez, Combined Raman scattering/photoluminescence analysis of Cu(In, Ga)Se_2 electrodeposited layers, Sol. Energy 103 (2014) 89.

[13] T. Nakada, Y. Hirabayashi, T. Tokado, D. Ohmori, T. Mise, Novel device structure for Cu(In, Ga)Se_2 thin film solar cells using transparent conducting oxide back and front contacts, Sol. Energy 77 (2004) 739.

[14] K. Durose, S.E. Asher, W. Jaegermann, D. Levi, B.E. McCandless, W. Metzger, H. Moutinho, P.D. Paulson, C.L. Perkins, J.R. Sites, G. Teeter, M. Terheggen, Physical characterization of thin-film solar cells, Prog. Photovolt. Res. Appl. 12 (2004) 177.

[15] B. Fernández, F. Claverie, C. Pécheyran, O.F.X. Donard, Direct analysis of solid samples by fs-LA-ICP-MS, Trends Anal. Chem. 26 (2007) 951.

[16] R.E. Russo, X. Mao, J.J. Gonzalez, V. Zorba, J. Yoo, Laser ablation in analytical chemistry, Anal. Chem. 85 (2013) 6162.

[17] R.E. Russo, X. Mao, H. Liu, J. Gonzalez, S.S. Mao, Laser ablation in analytical chemistry—a review, Talanta 57 (2002) 425.

[18] J.J. Gonzalez, D. Oropeza, X. Mao, R.E. Russo, Assessment of the precision and accuracy of thorium (^{232}Th) and uranium (^{238}U) measured by quadrupole based inductively coupled plasma-mass spectrometry using liquid nebulization, nanosecond and femtosecond laser ablation, J. Anal. At. Spectrom. 23 (2008) 229.

[19] C.A. Heinrich, T. Pettke, W.E. Halter, M. Aigner-Torres, A. Audetat, D. Gunther, B. Hattendorf, D. Bleiner, M. Guillong, I. Horn, Quantitative multi-element analysis of minerals, fluid and melt inclusions by laser-ablation inductively-coupled-plasma mass-spectrometry, Geochim. Cosmochim. Acta 67 (2003) 3473.

[20] T. Trejos, S. Montero, J.R. Almirall, Analysis and comparison of glass fragments by laser ablation inductively coupled plasma mass spectrometry (LA-ICP-MS) and ICP-MS, Anal. Bioanal. Chem. 376 (2003) 1255.

[21] M.D. Seltzer, K.H. Berry, Laser ablation ICP-MS profiling and semiquantitative determination of trace element concentrations in desert tortoise shells: documenting the uptake of elemental toxicants, Sci. Total Environ. 339 (2005) 253.

[22] V. Margetic, K. Niemax, R. Hergenröder, Application of femtosecond laser ablation time-of-flight mass spectrometry to in-depth multilayer analysis, Anal. Chem. 75 (2003) 3435.

[23] S.D. Müller, R.A. Diaz-Bone, J. Feliz, W. Goedecke, Detection of specific proteins by laser ablation inductively coupled plasma mass spectrometry (LA-ICP-MS) using gold cluster labelled antibodies, J. Anal. At. Spectrom. 20 (2005) 907.

[24] J.S. Becker, Inductively coupled plasma mass spectrometry (ICP-MS) and laser ablation ICP-MS for isotope analysis of long-lived radionuclides, Int. J. Mass Spectrom. 242 (2005) 183.

[25] S.H. Jeong, O.V. Borisov, J.H. Yoo, X.L. Mao, R.E. Russo, Effects of particle size distribution on inductively coupled plasma mass spectrometry signal intensity during laser ablation of glass samples, Anal. Chem. 71 (1999) 5123.

[26] C. Liu, X.L. Mao, S.S. Mao, X. Zeng, R. Greif, R.E. Russo, Nanosecond and femtosecond laser ablation of brass: particulate and ICPMS measurements, Anal. Chem. 76 (2004) 379.

[27] J. Gonzalez, S.H. Dundas, C. Liu, X. Mao, R.E. Russo, UV-femtosecond and nanosecond laser ablation-ICP-MS: internal and external repeatability, J. Anal. At. Spectrom. 21 (2006) 778.

[28] C.C. Garcia, H. Lindner, K. Niemax, Transport efficiency in femtosecond laser ablation inductively coupled plasma mass spectrometry applying ablation cells with short and long washout times, Spectrochim. Acta B 62 (2007) 13.

[29] S.H. Lee, C.K. Kim, J.H. In, H.S. Shim, S.H. Jeong, Selective removal of $CuIn_{1-x}Ga_xSe_2$ absorber layer with no edge melting using a nanosecond Nd: YAG laser, J. Phys. D. Appl. Phys. 46 (2013) 105502.

[30] J.J. Gonzalez, A. Fernandez, D. Oropeza, X. Mao, R.E. Russo, Femtosecond laser ablation: experimental study of the repetition rate influence on inductively coupled plasma mass spectrometry performance, Spectrochim. Acta B 63 (2008) 277.

[31] C.Y. Liu, X.L. Mao, J. Gonzalez, R.E. Russo, Study of particle size influence on laser ablation inductively coupled plasma spectrometry using an in-line cascade impactor, J. Anal. At. Spectrom. 20 (2005) 200.

[32] R.G. Brereton, Introduction to multivariate calibration in analytical chemistry, Analyst 125 (2000) 2125.

[33] A.M. Leach, G.M. Hieftje, Standardless semiquantitative analysis of metals using single-shot laser ablation inductively coupled plasma time-of-flight mass spectrometry, Anal. Chem. 73 (2001) 2959.

[34] J.N. Miller, J.C. Miller, Statistics and Chemometrics for Analytical Chemistry, fourth ed. Prentice Hall, England, 2001.